Computer Engineering and Intelligent Systems
ISSN 2222-1719 (Paper) ISSN 2222-2863 (Online)
Vol.7, No.8, 2016

Effect of Differential Code Biases on the GPS CORS Network: A Case Study of Egyptian Permanent GPS Network (EPGN)

Mohammed A. Abid[1, 2*], Ashraf Mousa[3], Mostafa Rabah[4], Mahmoud El mewafi[1], and Ahmed Awad.[1]

1- Faculty of Engineering, Mansoura University, Egypt.

2- Faculty of Engineering, Tikrit University, Iraq.

3- National Research Institute of Astronomy and Geophysics, Helwan, Egypt.

4- Benha Faculty of Engineering, Benha University, Egypt.

Abstract

The Global Positioning Satellite System (GPS) Continuously Operating Reference Stations (CORS) are popular and have become increasingly dense throughout the world. One of the important factors affecting the GPS accuracy is the ionosphere Total Electron Content (TEC). The hardware Differential Code Biases (DCB), inherited in both Global Positioning System satellites and receivers, influence the total electron content estimation accuracy. DCB can be estimated using GPS data themselves or during the GPS data processing.

The effect of DCB on CORS results are studied here using nine CORS stations from the Egyptian Permanent GPS Net (EPGN). Bernese software version 5.0 is used for data analysis. Three strategies are applied to the data. The first strategy is using a special MATLAB code to estimate DCB which in turn is introduced as known input in Bernese. Using Bernese itself to estimate the DCB along with the ionosphere is the second method. The third way is to totally ignore the DCB. The three solutions are compared based on ratio of ambiguity resolutions, standard deviations, error ellipse, and closure errors.

The results indicate that the worst solution is obtained when ignoring the DCB. Both Bernese estimation and known DCB solutions are similar and gives good results. For example, the ratio of un-resolved ambiguity for baseline between Marsa-Alam and Arish is about 0.3096 for Bernese estimated DCB while it is about 0.5643 when ignoring DCB. Hence it is recommended to consider the DCB when processing GPS data for precise applications.

1. Introduction

The CORS are now widely spread all over the world. The ground-based dual-frequency GPS observations are affected severely by the ionosphere. For all precise CORS applications which are supported by code observation data, existing code (or pseudorange) biases represent a non-negligible error source. This includes “time-oriented” applications such as high-precision GPS satellite clock estimation as well as time transfer among GPS observing stations. To accurately mitigate the ionospheric error effect on GPS solution, the DCB need to be compensated (Dach et al., 2007).

DCB have three main components; the differential code bias of the satellite (SDCB) and receiver (RDCB) and the difference between delays on L1 and L2 frequencies. SDCB and RDCB biases magnitude range from several nano-seconds to tens of nano-seconds. In the current research, SDCB are dealt with through the IGS values. The current research concentrates on The RDCB and L1, L2 delay differences effect. The RDCB depends on the type of observation and the characteristics of the hardware. Receiver DCB can be constant over several days under rather smooth ionospheric conditions. But in certain areas with great ionosphere variations such as equatorial or auroral zones, the constant assumption could not always be true (Raju, 2005).

The dual frequency GPS code and carrier phase measurements in meters can be described by the following equations (subscript i = 1, 2, refers to GPS frequencies, f_1 and f_2) (Sunehra, 2016, Misra and Enge, 2001):

$$P_i = \rho + c(dt_u - dt^s) + TD + I_i + Sdcb_{Pi} - Rdcb_{Pi} + \varepsilon(P_i) \quad (1)$$

$$L_i = \rho + c(dt_u - dt^s) + TD - I_i + SDCB_{Li} - RDCB_{Li} + \lambda_i N_i + \varepsilon(L_i) \quad (2)$$

Where ρ is the true geometric range (m); c is the speed of light (m/s); dt_u, dt^s are the receiver and satellite clock offsets, respectively (s); TD is the tropospheric delay (m); I_i is the ionospheric delay at frequency f_i (m); $Sdcb_{Pi}$ and $Rdcb_{Pi}$ are the satellite and receiver instrumental group delay biases at frequency f_i , respectively (m); $SDCB_{Li}$ and $RDCB_{Li}$ are the satellite and receiver instrumental phase delay biases at frequency fi, respectively (m); λ_i is the carrier wavelength at frequency f_i (m); N_i is the carrier phase integer ambiguity (cycles); ε(.) includes measurement noise and multipath error (m).The DCB effect and estimation is carried out based on the above two equations.

To investigate effect of DCB on GPS solution results, nine stations of the Egyptian Permanent GPS net (EPGN) as data source are used. Data analysis is carried out using Bernese software version 5.0. To study the effect of DCB on the GPS results the data are processed using three different strategies. The first processing way is using a special MATLAB code to estimate DCB. The estimated DCB values are considered as known input in Bernese. The second strategy use Bernese software to estimate the DCB along with the local ionosphere. Ignoring the DCB in the solution is the third method. The results of the three strategies solutions are compared to find the best strategy. The criteria used here to evaluate the three solutions are based on ratio of ambiguity resolutions, standard deviations, error ellipse, and closure errors.

As is expected, the results show that ignoring the DCB gives the worst solution. Bernese estimation and MATLAB estimated DCB solutions give nearly the same good results. For example, the ratio of un- resolved ambiguity for baseline between Marsa Alam and Arish is about 0.3096 for Bernese estimated DCB while it is about 0.5643 when ignoring DCB. Hence it is recommended to consider the DCB when processing GPS data for precision applications.

2. Data

Nine stations GPS of EPGN sites were used in the current research. Stations that have long time stable record; located in the same tectonic plate in EGYPT and belonging to EPGN EGYPT reference Frame Permanent Network are selected here. Figure (1) shows the map featuring the nine GPS stations. Table (1) shows the Cartesian coordinates of the nine stations. The network covers an area of about 947 km by 484 km in latitude and longitude approximately. Data are collected using two different Trimble model receivers; Trimble 5700 and Trimble NETR5. Both receivers provide non correlated C1 and P2 observation data. The data used covers about one year, where every month was represented by three days. The data was in Receiver Independent Exchange format (RINEX) format with one second sampling rate. The elevation cut-off angle of 3° was used for the collected data. The precise ephemeris (SP3) and ionospheric models are taken from IGS.

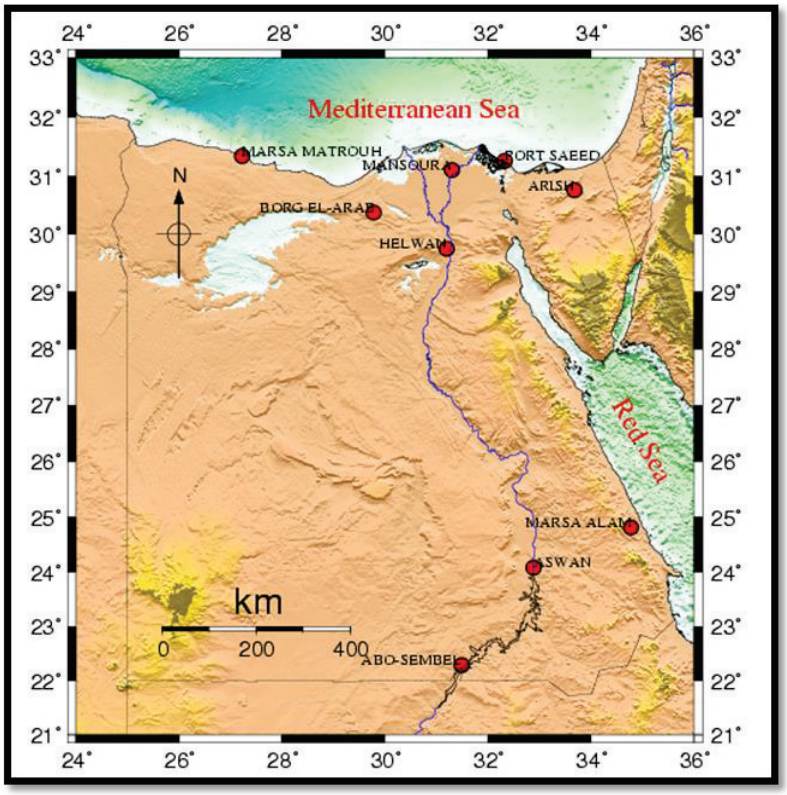

Figure 1. Location of the used GPS station

The selected baselines distances range from 94 (MNSR-SAID) to 1069 (MTRH-ABSM) km. A daily receiver DCB values as well as their mean for three days in each month during one year were computed.

Table1. Cartesian coordinates of the GPS sites.

Station Id.	X(m)	Y(m)	Z(m)
PHLW	4728141.2348	2879662.6041	3157147.1275
MNSR	4671006.2282	2845893.5711	0269812.0787
SAID	4612664.2381	2917621.3718	3289234.9243
BORG	4765954.3185	2704546.1674	3252949.1622
ARSH	4551743.5738	3026108.3528	3276117.4525
MTRH	4847946.8930	2494773.3017	298721.2242
ASWN	4899061.5611	3163086.8817	2575414.1543
ABSM	5024945.1535	3084578.9769	2424694.7180
ALAM	4742516.3847	3305688.9798	2685814.2467

3. Data Analysis

Data analysis is carried out using Bernese version 5.0 (Dach et al. 2007). The Bernese processing was set up to: elevation cut-off at 3°; *Quasi*-Ionosphere-Free (QIF) algorithm in baseline mode as ambiguity resolution strategy; ionosphere-free linear combination to mitigate ionosphere dispersion; Saastamoinen tropospheric model and no ocean loading. The IGS final orbits; and Earth Rotation Parameter files from IGS data center

(ftp://igs.ifag.de) are used. Figure (2) presents a synthetic flow chart with input and output data for processing using Bernese software.

The data analysis starts with preprocessing. The processing is similar for the three strategies used here for most of the steps. The differences between the three strategies are in the processing part of the software (figure 2). In the 1st strategy, the DCB is totally ignored and its term in equation 1 and 2 above is removed. Using the MATLAB script results ((Sedeek et al., 2015), (Mohammed et al., 2016)) to substitute the DCB in both equations is the second method of processing. Assuming DCB as unknown in the Bernese processing is the way to deal with DCB in the third strategy. To investigate the effect of DCB and to choose the best solution strategy, many parameters are used for this purpose. The parameters include precision (RMS and Error ellipse), ambiguity resolution success rate and closure error.

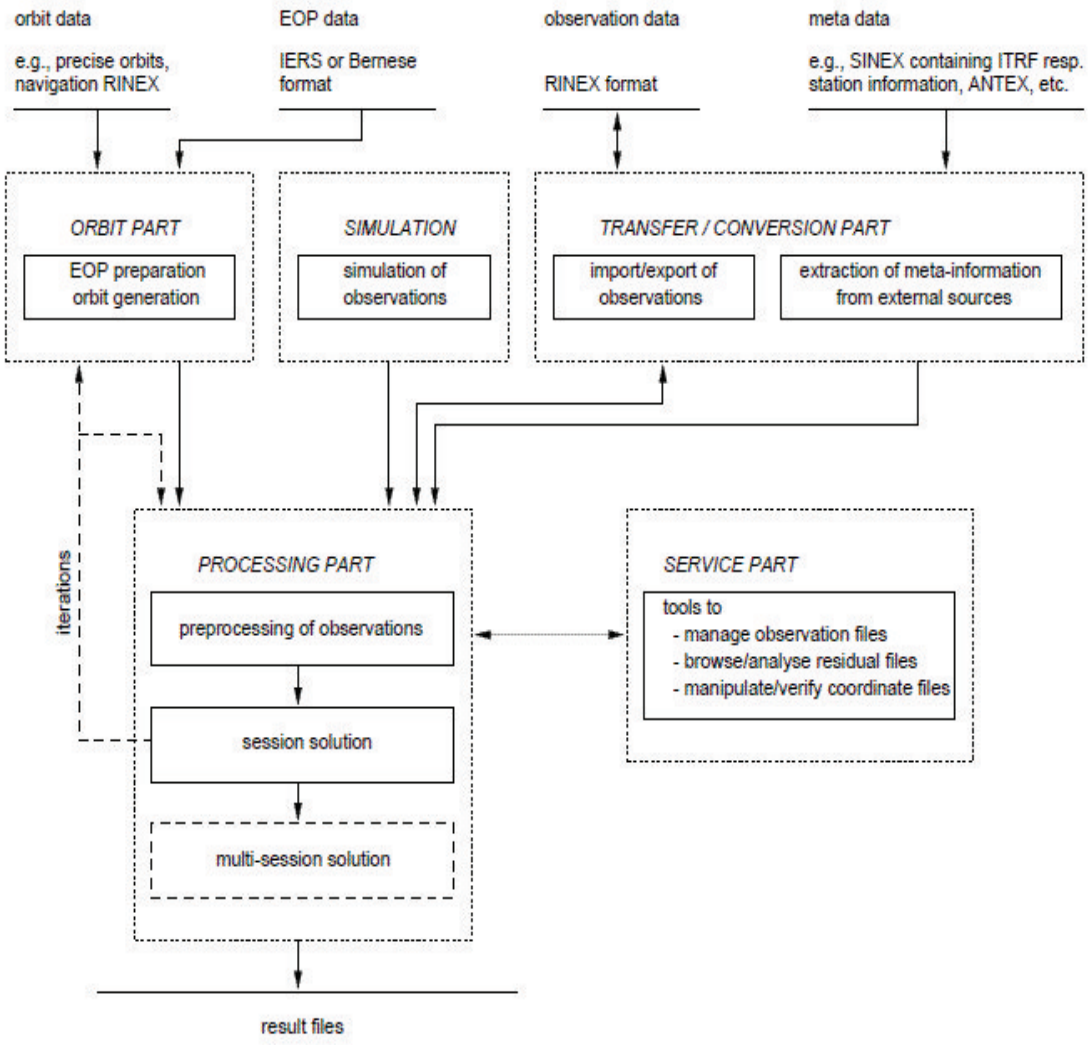

Figure 2. Functional flow diagram of standard processing in Bernese GPS Software

4. Results and discussion

In order to study the effect of DCB on the network solution, three cases are investigated as explained before. As stated above, the investigations will consider RMS of the coordinates, loop closure, coordinates error ellipse and ambiguity resolution to compare the results of the three cases.

The lower part of figures (3) to (11) show the effect of DCB on X coordinates RMS for the three solution cases at the selected stations for the whole year. The range minimum-to-maxim RMS value with DCB estimated by m-code is from 0.0092m at MTRH to 0.0148m at ARSH, while it is from 0.0092 m at MTRH to 0.014 m at ARSH when ignoring DCB. RMS values for estimation of DCB with Bernese change from 0.009m at MNSR and ALAM to 0.0137m at MNSR. Generally all three cases show almost the same RMS and the change of RMS is about 0.005 m. The changes of Y coordinates RMS are given in middle part Figures 3 to 11. The range minimum-to-maxim RMS value with DCB estimated by M-code is from 0.0065m at ASWN to 0.0114m at ARSH, while it varies from 0.0064 m at BORG to 0.01301 m at MNSR when ignoring DCB. RMS values for estimation of DCB with Bernese changes from 0.0062m at ALAM to 0.01m at PHLW. Y coordinates RMS shows similar minimum value for all three cases. This minimum value is about 0.006 m. The Bernese estimated DCB shows the lowest value of the maximum RMS of 0.01 m while highest value is about 0.013 m is given when ignoring DCB case.

The temporal variations of the Z coordinates RMS are given in upper part of Figures 3 to 11. The range minimum-to-maxim RMS value with DCB estimated by M-code is from 0.0042m at ARSH to 0.0091m at PHLW and MNSR, while it is ranges from 0.0042 m at ARSH to 0.0092 m at MNSR when ignoring DCB. RMS values for estimation of DCB with Bernese changes from 0.004 m at ARSH to 0.009 m at PHLW and MNSR. Generally all three cases show almost the same RMS and the change of RMS is about 0.005 m.

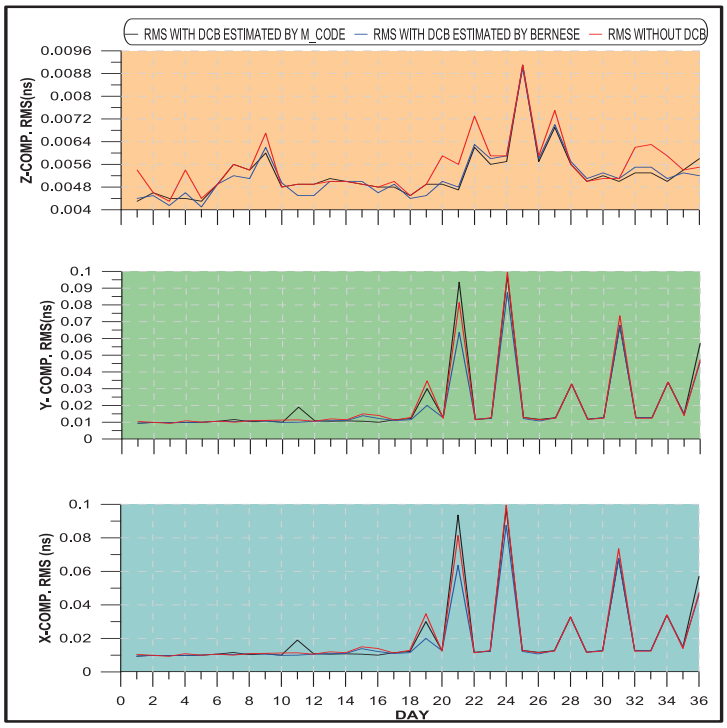

Figure 3. RMS in X, Y, Z, Axis for ABSM station in 36 day

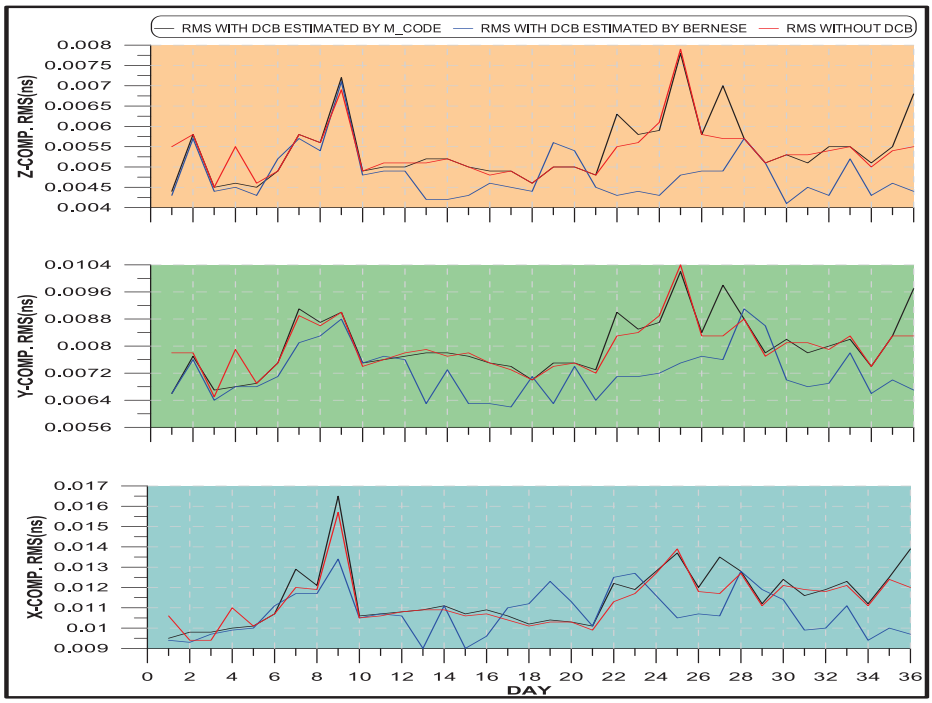

Figure 4. RMS in X, Y, Z, Axis for ALAM station in 36 day

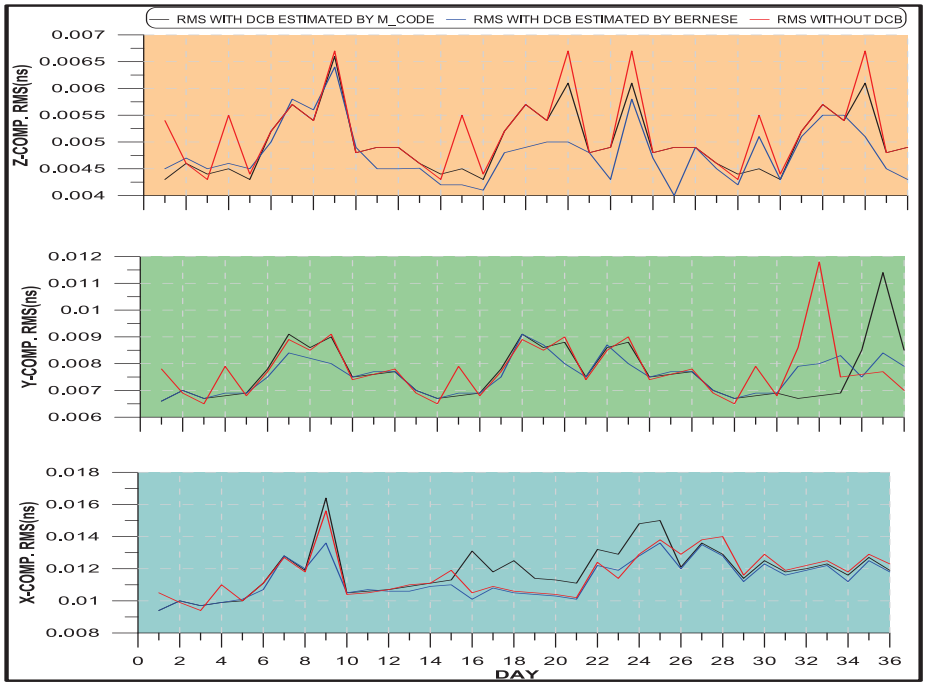

Figure 5. RMS in X, Y, Z, Axis for ARSH station in 36 day

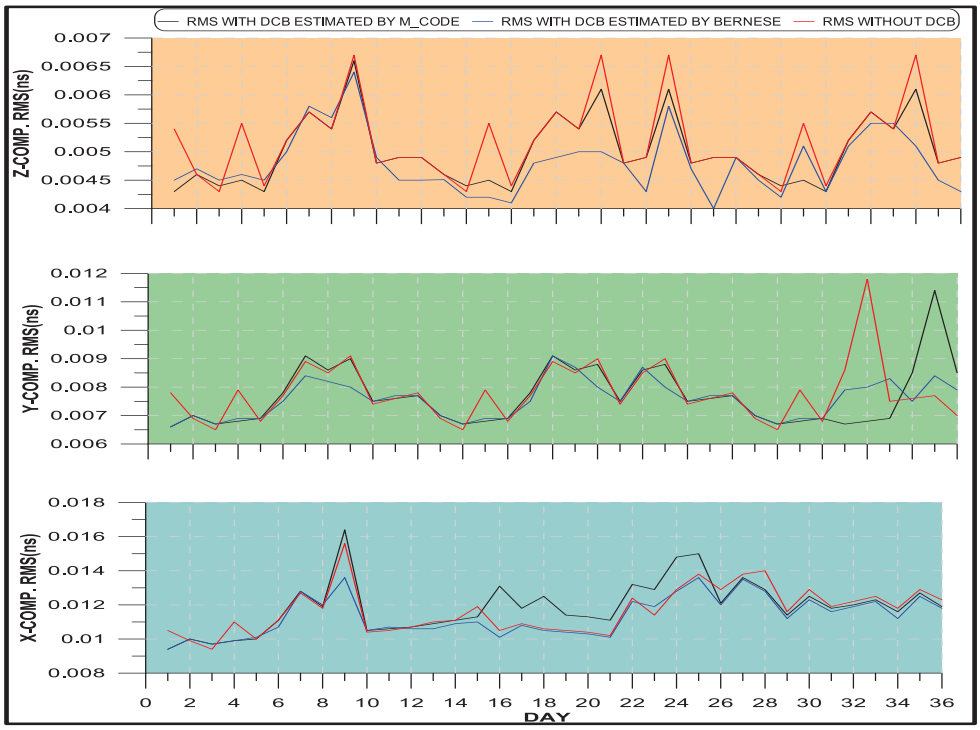

Figure 6. RMS in X, Y, Z, Axis for ASWN station in 36 day

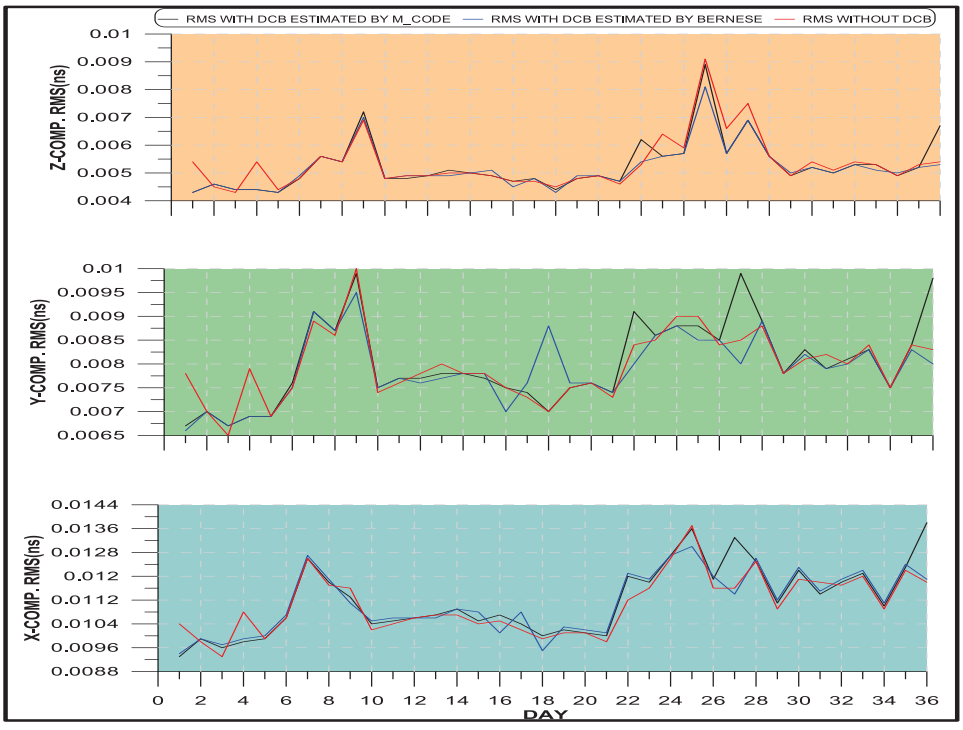

Figure 7. RMS in X, Y, Z, Axis for BORG station in 36 day

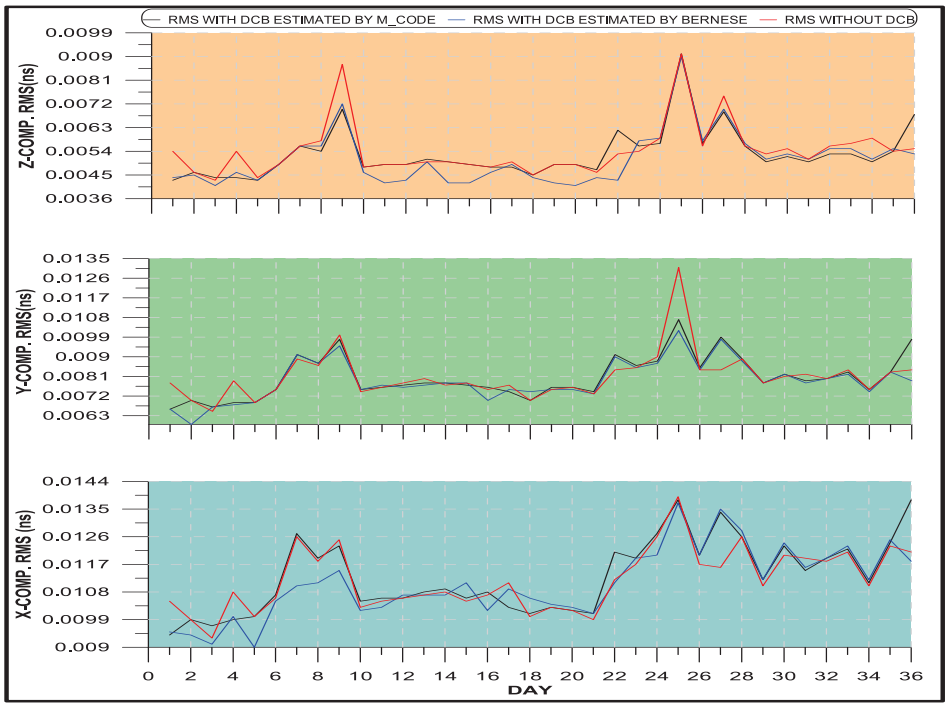

Figure 8. RMS in X, Y, Z, Axis for MNSR station in 36 day

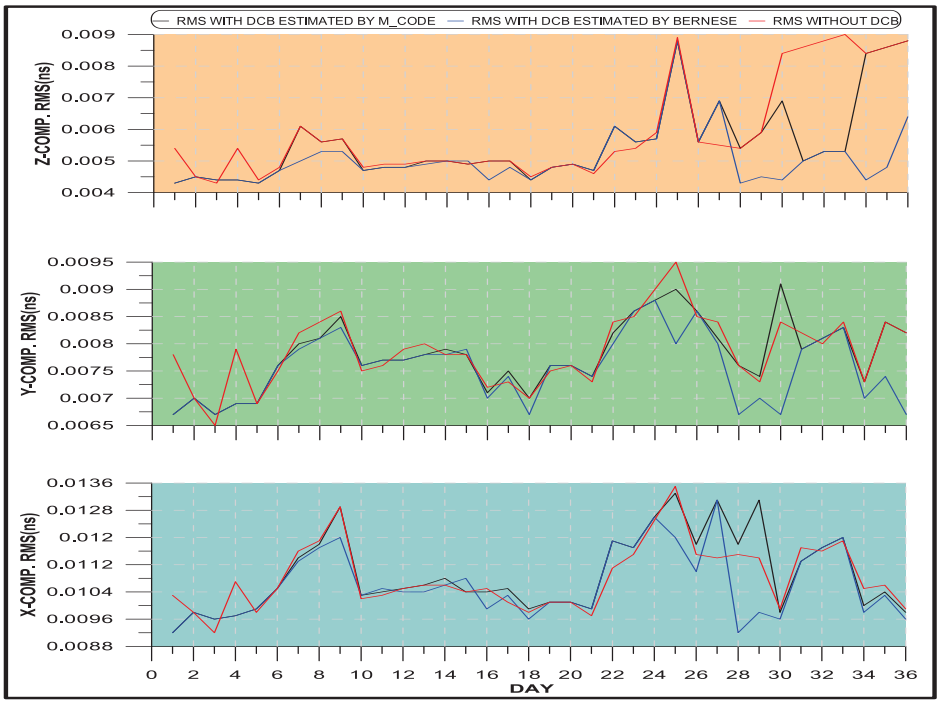

Figure 9. RMS in X, Y, Z, Axis for MTRH station in 36 day

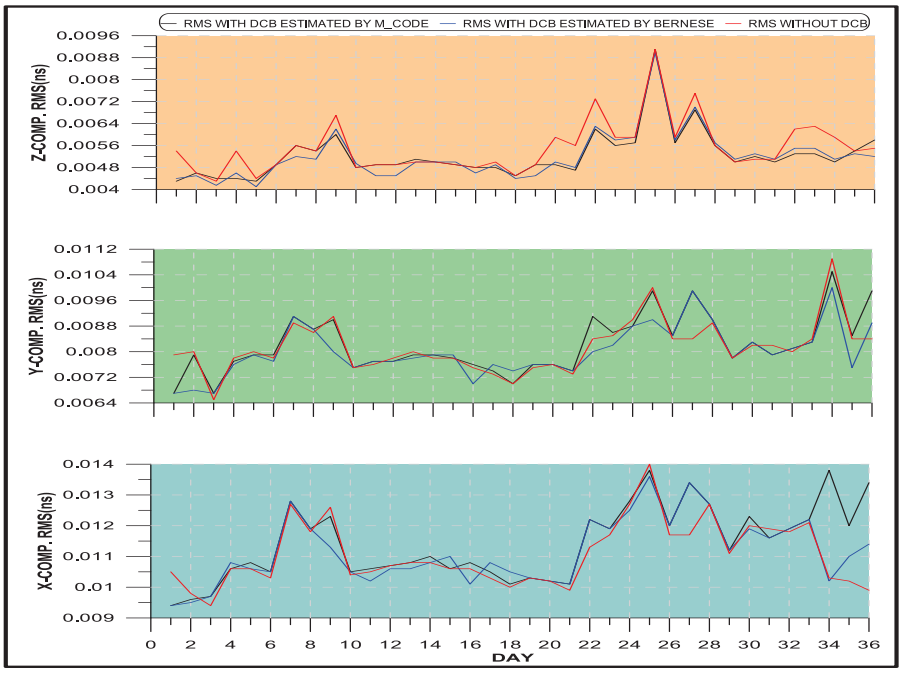

Figure 10. RMS in X, Y, Z, Axis for PHLW station in 36 day

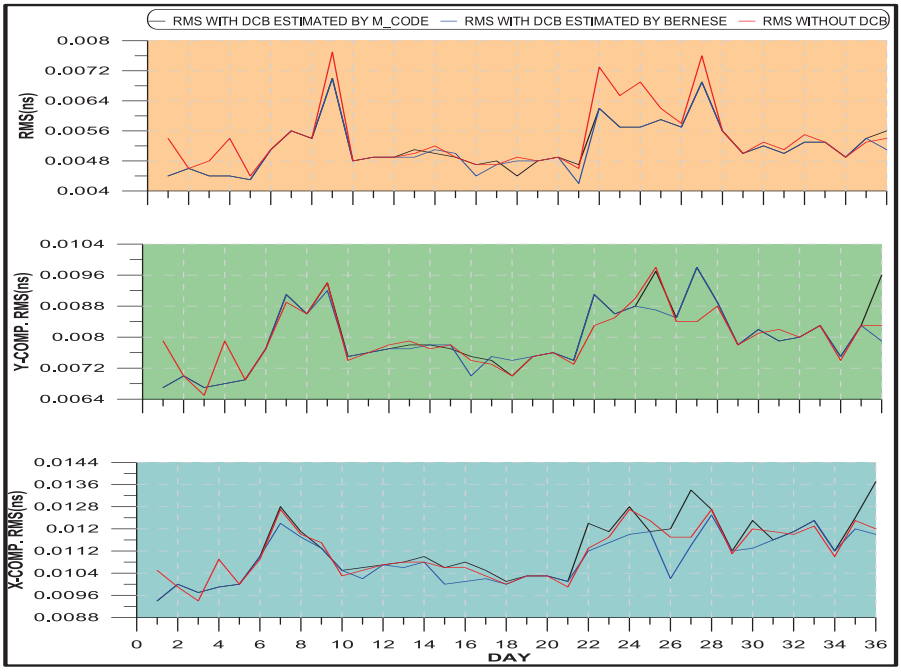

Figure 11. RMS in X, Y, Z, Axis for SAID station in 36 day

The second test used here is the loop closure error. Figure (12) shows the used six loops. These loops are selected to give different stations, loop length and height difference among the loop. Figure (13) represent the change of loop closure with average height of the loop stations. The closure error seems to be increased with the average height of the loop. The figure indicates that the m-code strategy is the best strategy compared with the other two strategies. The loop closure difference is about 1-2 mm between the m-code and ignoring DCB case for most of the heights. It increases gradually with heights to about 3.5 mm for the 115 m height case.

The change of loop closure with height differences among the loop is given in figure (14). The m-code strategy assumes the best (minimum) results of closure error. Bernese case is very similar to the m-code case for most height differences. The m-code loop closure ranges from 0.0015 to 0.0025 m. The worst case is shown when ignoring the DCB. The values for this last case change from 0.0022 to 0.0065 m.

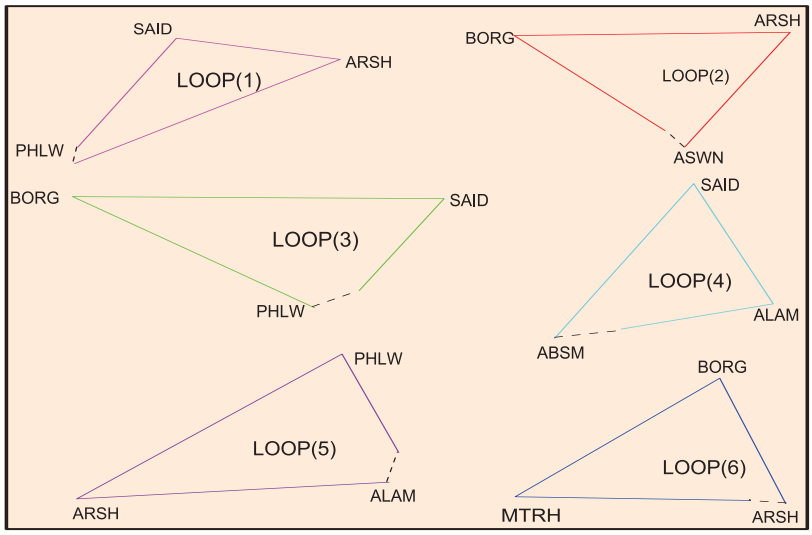

Figure 12. Shape of the six loops

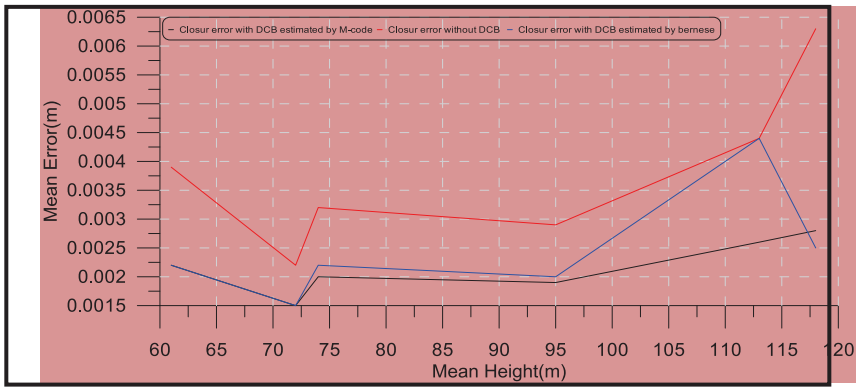

Figure 13. Mean closure errors estimated from six loop and mean height

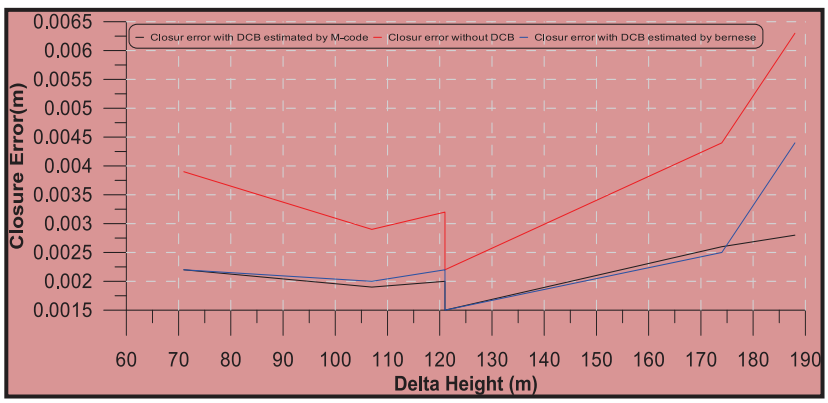

Figure 14. Delta height with closure error (m)

It is clear from figure (15) and table (2) that the loop closure increases systematically with the loop length. The Bernese estimated DCB case and m-code estimated case show similar closure errors except for the loop ASWN-BORG-SAID-ASWN. For this loop Bernese case shows bad results compared to m-code case. The table shows that the case when ignoring the DCB gives the highest loop closure errors. It is worth noting that the loop closure error ranges from 0.0015 to 0.0028 m for m-code estimated DCB case.

Table 2. Closure estimated by three different ways

Loop	Length(km)	Closure error for M-code DCB estimated (m)	Closure error for ignoring DCB(m)	Closure error for Bernese estimated DCB (m)
ASWN-BORG-ARSH-ASWN	562	0.0015	0.0022	0.0015
PHLW-SAID-ARSH-PHLW	646	0.0019	0.0029	0.002
ALAM-PHLW-ARSH-ALAM	1224	0.002	0.0032	0.0022
ARSH-MTRH-BORG-ARSH	1605	0.0022	0.0039	0.0022
PHLW-BORG-SAID-PHLW	1900	0.0026	0.0044	0.0025
ASWN-BORG-SAID-ASWN	2008	0.0028	0.0063	0.0044

The loop closure varies from 0.0022 to 0.0063 m when ignoring DCB. The loop closure range as 0.0015 to 0.0044 m for the Bernese estimated DCB strategy.

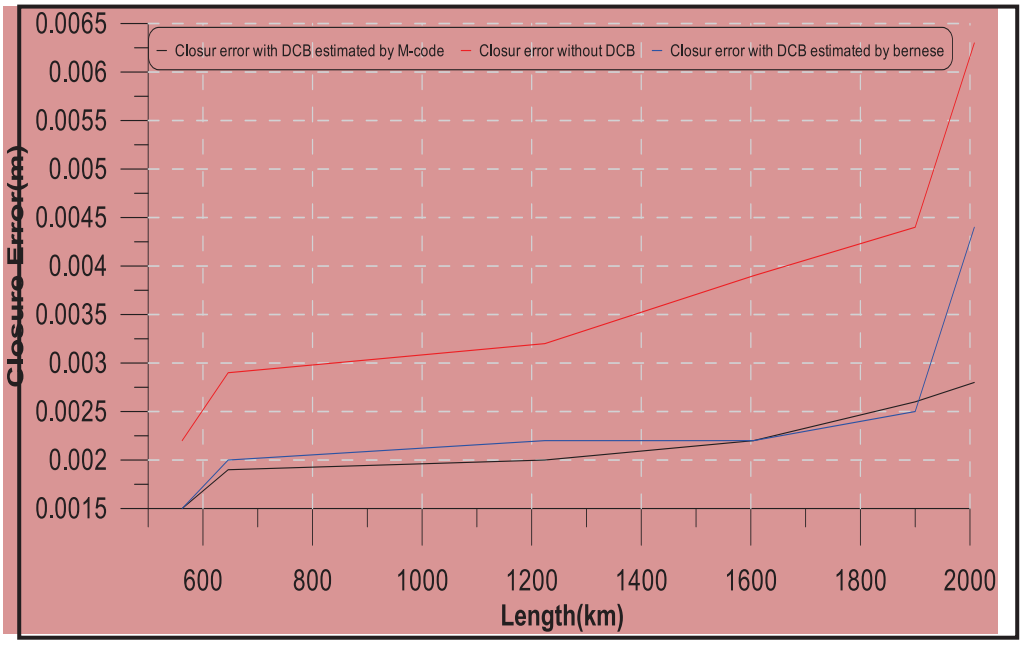

Figure 15. Length with closure error

Figures (16) to (18) represent the error ellipse results of the EPGN stations for the three solution strategies. Table (3) shows the detailed results of the error ellipse concerning error ellipse semi-major (a), semi-minor (b) axis and its orientation angle (δ). It is clear that both Bernese Software 5.0 estimated and M-code estimated DCB cases gives very similar results regardless of the station. The error ellipse parameters assume larger values for the case when ignoring DCB totally.

Table 3. Ellipsoid error estimated by three different ways

Station	Long°.	Lat°.	M _code			Without DCB			Bernese Software 5.0		
			a	b	δ	a	b	δ	a	b	δ
ABSM	31.54	22.49	4.01	4.3	82.5	4.8	5.6	65.7	4.1	4.4	82.5
ASWN	32.85	23.97	4.1	4.5	92.7	4.9	5.7	73.3	4.8	5.2	92
ALAM	34.88	25.07	4	4.6	103.3	5	5.8	82.8	5.1	6	104
PHLW	31.34	29.86	4.02	5.2	86.9	4.9	6.4	78	5.1	6.8	88
BORG	29.57	30.86	4	5.4	81.3	4.8	6.6	74.3	4.7	7.1	81.6
MNSR	31.35	31.04	4.03	5.4	87.2	4.9	6.6	79.2	5.6	6	87
ARSH	33.62	31.11	4.05	5.4	94.4	4.9	6.6	85.4	5.5	7.4	93.2
SAID	32.31	31.24	4	5.4	90.4	4.9	6.6	81.8	4.8	6.6	90.3
MTRH	27.23	31.34	4.01	5.5	74.5	4.8	6.7	69.2	4.1	5.6	74.5

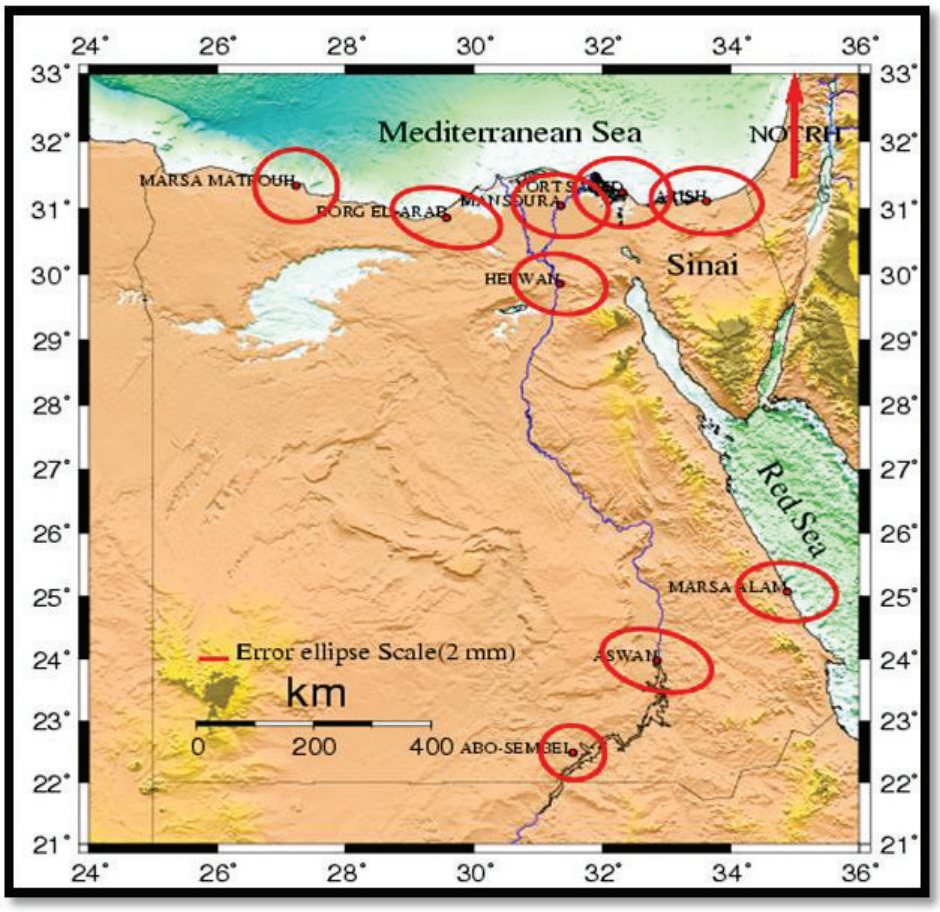

Figure 16. Ellipse error with DCB estimated by M_code

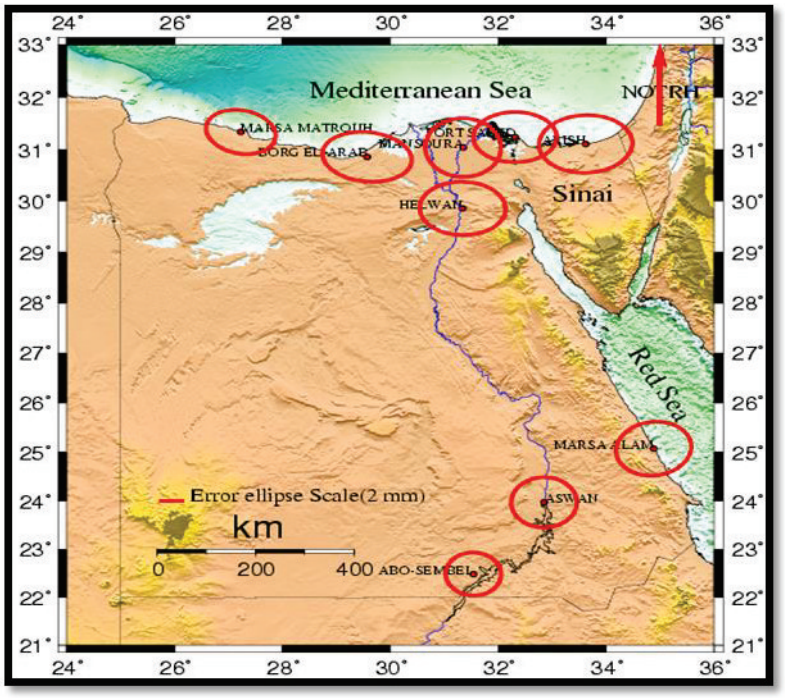

Figure 17. Ellipse errer with DCB estimated by Bernese

The two figures (19) and (20) stipulate the changes of the error ellipse size with latitude and longitude of the EPGN stations. It is clear from figure (35) that the m-code shows the minimum values of the error ellipse size. The worst case is shown for the error ellipse size when ignoring the DCB. The error ellipse size nearly increases with latitude. On the other hand, figure (36) indicates that the error ellipse size does not show clear trend with the longitude.

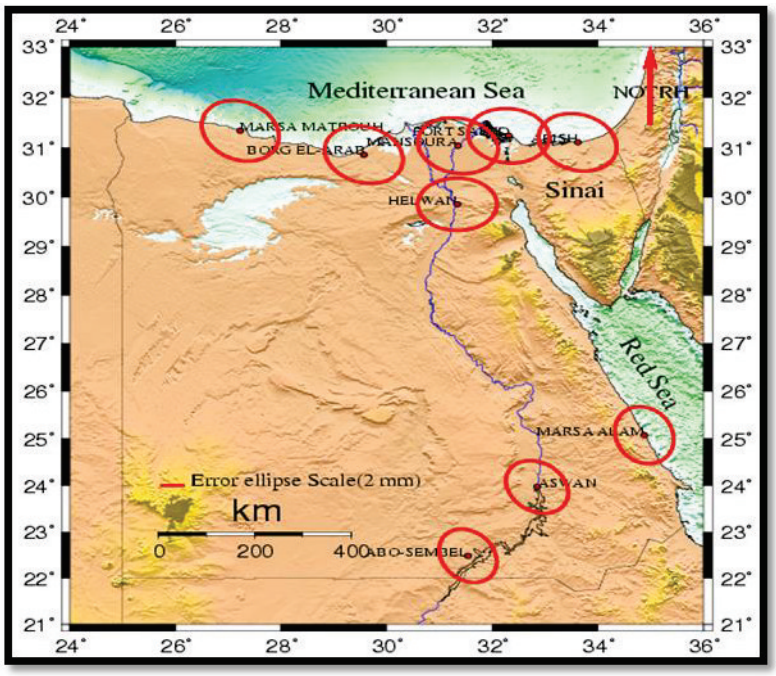

Figure 18. Ellipse errer without using DCB

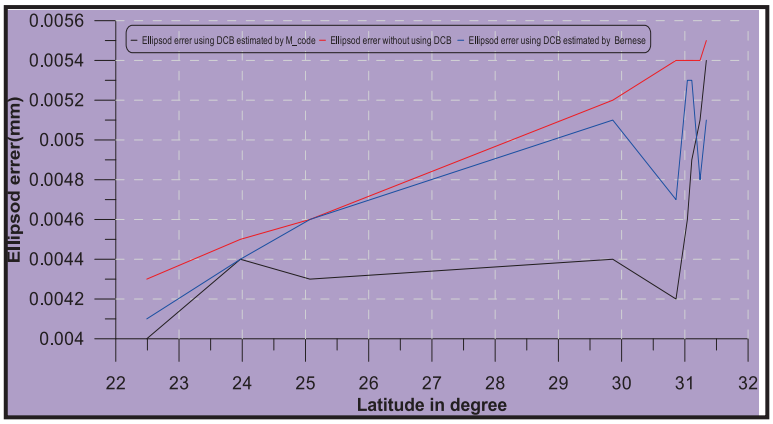

Figure 19. The relation between ellipsoid error and latitude

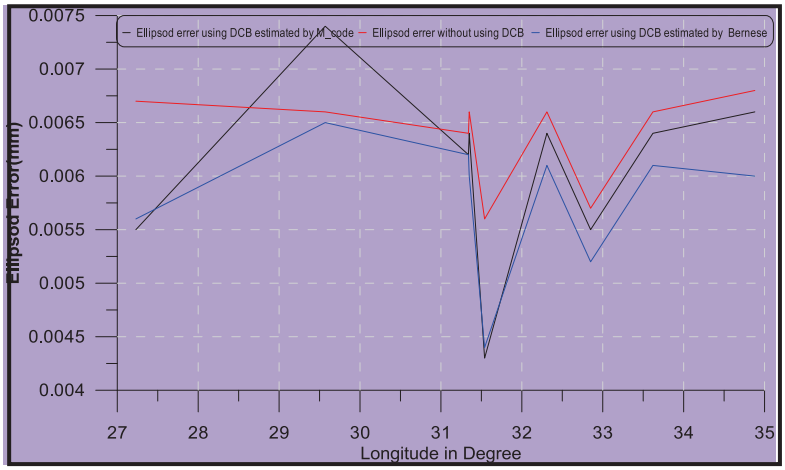

Figure 20. The relation between ellipsoid error and longitude

Figure (21) shows the effect of DCB on ambiguity ratio for the three solution cases at the selected stations and the relation between ambiguity ratio and length. The range minimum-to-maxim ambiguity value with DCB estimated by m-code is from 0.3196 at base line ALAM-ARSH to 0.5573 at base line ARSH-MNSR, while it is from 0.3380 at base line ALAM-ARSH to 0.5643 at base line ARSH-MNSR when ignoring DCB. Ambiguity ratio value estimation of DCB with Bernese changes from 0.3096 at base line ALAM-ARSH to 0.5545 at ARSH_MNSR base line. Generally values of ambiguity ratio when estimation of DCB with Bernese is better values than the other two cases.

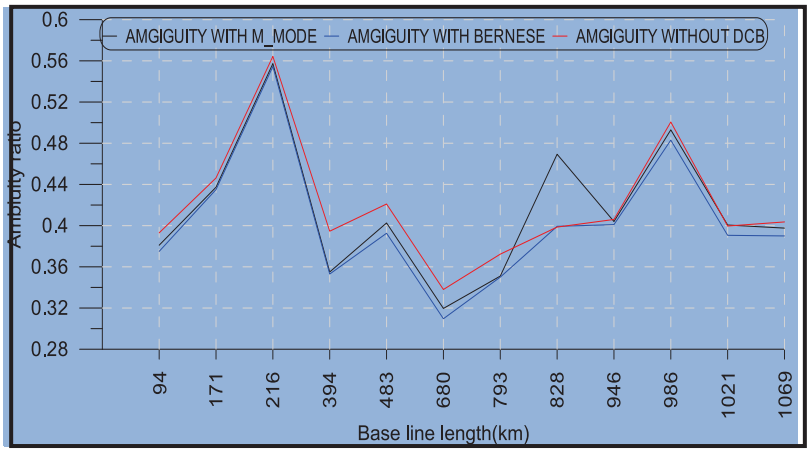

Figure 21. Ambiguity ratio with length

5. Conclusions

In this paper, three prominent techniques are used for studying the effect of DCB. The so called m-code and Bernese strategies were based on the introduction of DCB Delays calculated from GPS data. While ignoring DCB discard the effect of DCB totally. For this study, many GPS baselines belonging to EPGN permanent stations in EGYPT were used. Ratio of ambiguity resolved, closure error, ellipse error and standard deviation are used to compare the three solution strategies and to find the best technique to process EPGN data.

Ignoring the DCB totally produces the least accurate results. The other two strategies give much more accurate results. The difference between all strategies is generally at the millimeters level. Comparing Ignoring DCB case

with other two strategies gives differences reach up to sub centimeters level. Using DCB as known values or estimating it leads to a more precise coordinate estimation. In order to enable the permanent station users to get high accuracy, it is recommended to take DCB errors into account either by getting them for IGS or by special estimation algorithm.

Acknowledgments

We would like to express our sincere thanks to the staff of crustal movement Lab., Geodynamic department of NRIAG for providing GPS data used in the current research. Also, we would like to express our gratitude to the staff of public work department, civil Engineering, Mansoura University for the good research environment. This research is supported by Tikrit University, the Iraqi Ministry of Higher Education- Baghdad- Republic of Iraq.

Reference

Choi B.K., Chung J.K., and Cho J.H., (2010), Receiver DCB Estimation and Analysis by Types of GPS Receiver, J. Astron. Space Sci. 27(2), 123-128 (2010)

Dach R., Hugentobler U., Fridez P. and Meindl M., (2007), *Bernese GPS Software Version 5.0*, AIUB Astronomical Institute, University of Bern.

Kao S. P., Chen Y. C., and Ning F. S., (2013), A MARS-based method for estimating regional 2-D ionospheric VTEC and receiver differential code bias, Advances in Space Research 53 (2014) 190–200.

Klobuchar J. A., (1987), Ionospheric time-delay algorithm for single frequency GPS users, IEEE Trans. Aerosp. Electron. Syst. AES-23 (3), 325–331.

Misra P. and Enge P., (2001), Global Positioning System Signals Measurements, and Performance. Ganga Jamuna Press, MA.

Mohammed A. Abid, A. Mousa, M. Rabah, M. Mewafi, and A. Awad., (2016), Temporal and Spatial Variation of Differential Code Biases: A case study of regional network in Egypt, Alexandria Engineering Journal Vol. 55, 1507-1514.

Raju P. L. N., (2005), FUNDAMENTALS OF GPS, *Geoinformatics Division Indian Institute of Remote Sensing, Dehra Dun*

Sedeek A. A., Doma M. I., Rabah M., and Hamama M. A., (2015), Determination of Zero Difference GPS Differential Code Biases for Satellites and Prominent Receiver Types, under publishing in Arab Journal of Geoscience, Springer.

Sunehra, D., (2016), TEC and Instrumental Bias Estimation of GAGAN Station Using Kalman Filter and SCORE Algorithm, positioning Vol. 7, 41-50 pp.